Probing the ^{6}Li cluster structure with alpha-particle elastic scattering

B.A. Urazbekov[1,2], A.S. Denikin[1,3]

[1]Joint Institute for Nuclear Research, Dubna, Russia

[2]Institute of nuclear physics, Almaty, Kazakhstan

[3]Dubna state university, Dubna, Russia

E-mail: bakytzhan.urazbekov@gmail.com

The three-body model $\alpha + n + p$ for ^{6}Li is applied as a probe with elastic scattering of α-particles. Elastic scattering is described within the optical model framework, while the rising of the cross section at the backward scattering angles is treated by means of an approximation of the np transfer mechanism. Both parts of the optical potential are obtained by fitting the depths of the same folding potentials to experimental data. The folding potential, in turn, is based on the three body-wave function of ^{6}Li. Spectroscopic amplitudes for the np cluster are extracted in calculations based on the CRC method. One-step and two-step transfer mechanisms are taken into account for the np transfer mechanism. The calculation results indicate the dominance of the one-step mechanism over the two-step transfer mechanism of the np cluster.

Keywords: elastic scattering; elastic transfer; three-body model

Introduction

Light atomic nuclei can create nucleon associations often called clusters. The clusters in atomic nuclei can be the simplest particles: d, t, ^{3}He, and α. Since the α-particle has a large binding energy 28.29 MeV compared to other clusters, it remains the most likely cluster type that is formed from the simplest particles.

The nucleus ^{6}Li is a good example in terms of probing cluster models. The structure was studied by means of the stochastic variational method [1, 2], hyperspherical harmonics [3, 4], and no-core shell model [5, 6] approaches. In particular, the cigar-like and helicopter-like geometrical configurations were revealed within

the three body model framework in [1, 3]. Moreover, in this work the ground state properties, electromagnetic static characteristics of ^{6}Li, and the spectroscopic factor of the $\alpha + d$ configuration in ^{6}Li were calculated.

The structure of ^{6}Li was also studied via nuclear reactions [7]. Within the Distorted wave Born approximation (DWBA) and Coupled Reaction Channels (CRC) methods the spectroscopic factor of $\alpha + d$ in ^{6}Li was obtained [8]. By means of the CRC calculations, the deformation parameter and the spectroscopic amplitudes were also extracted [9, 10].

Elastic scattering of α particles on ^{6}Li at a laboratory energy 166 MeV was investigated in Ref. [11]. An anomaly was detected as a rising in the differential cross section at backward scattering angles, and it was treated by the elastic transfer of the np-cluster. Using the wave function built up with the hyper-spherical harmonics approach, the authors could gain good agreement of the calculated cross section with experimental data in the entire range of angles.

The aim of this work is to study the elastic scattering of α-particles on ^{6}Li in matters of the three body model $\alpha + p + n$. This work proposes alternative methods to study the elastic scattering $\alpha + {}^6$Li in relation with Ref. [11]. To do this, the previously developed theoretical method [12, 13] should be applied, which was also used in the ^{3}He $+{}^9$Be nuclear reactions [14]. The calculation of the double-folding potential for the $\alpha + {}^6$Li system and the implementation of the two-step transfer of the np-cluster are the novelty of the current work.

In this work, the elastic scattering is treated within the Optical model (OM). Both real and imaginary parts of the Optical potentials (OP) are executed by the Double-folding (DF) potential. For the purposes of making the calculations more realistic, the density distribution function of the nuclear matter of ^{6}Li, as part of the DF potential, is obtained on the basis of the three body wave function. In the first section, brief theoretical methods are given about the density distribution function of nuclear matter, and DF potential. A more detailed description of the density function using the three body wave function can be found in Refs. [13, 15], and of the double folding model see Refs. [16, 17]. In the second section the results and discussions are given. Lastly, the conclusions are drawn at the end.

Theoretical method

The density distribution function

The density distribution function of nuclear matter of ^{6}Li within the three body model can be expressed as follows:

$$\rho_{Li}(\mathbf{R}) = \sum_{k=\{\alpha np\}} \rho_k(\mathbf{R}),\qquad(1)$$

where the sum goes over all the clusters $k = \{\alpha, n, p\}$ in ^{6}Li. The density function of the cluster k can have

$$\rho_k(\mathbf{R}) = \langle\, \Psi_{tot}^{JM} \mid \hat{\rho}_k \mid \Psi_{tot}^{JM} \,\rangle,\qquad(2)$$

here, Ψ_{tot}^{JM} is the total wave function of ^{6}Li, which is built up on the basis of the Gaussian functions by means of the Stochastic variational method [1]. The operator of the density function $\hat{\rho}_k$ is defined as

$$\hat{\rho}_k \equiv \begin{cases} \delta\left(\mathbf{y}_k - y_0^{(k)}\mathbf{R}\right), & \text{for } k\text{-th nucleons,} \\ \rho_\alpha\left(\mathbf{y}_\alpha - y_0^{(\alpha)}\mathbf{R}\right), & \text{for } \alpha\text{-cluster,} \end{cases} \tag{3}$$

where $\mathbf{y}_k$ is the Jacobi coordinate between the α-cluster and the center of masses of the np-cluster, $\mathbf{R}$ is the radius from the cm of ^{6}Li, and $\delta(\mathbf{z})$ is the delta function. The internal density distribution function of the α-cluster $\rho_\alpha(\mathbf{r})$ can take the form:

$$\rho_\alpha(\mathbf{x}) = \rho_0 \exp\left(-\gamma_0 \mathbf{x}^2\right). \tag{4}$$

Provided the function $\rho_\alpha(\mathbf{x})$ is normalized to unity, its parameters have

$$\gamma_0 = \frac{3}{2}\frac{1}{<r_\alpha^2>}, \quad \rho_0 = \left(\frac{\gamma_0}{\pi}\right)^{\frac{3}{2}}. \tag{5}$$

Here, the square root of $<r_\alpha^2>$ is the rms matter radius of the α-particle, which can be equal to $1.461\ fm$ [16].

Optical potential

The numerical calculations of elastic scattering can be performed in the framework of the OM with the optical potential given by:

$$U(r) = -V^V(r) - iW^V(r) + V^C(r), \tag{6}$$

where r is the distance between the α-projectile and ^{6}Li, and V^V, W^V, V^C are the real volume, imaginary volume, and Coulomb potentials, respectively. The volume potentials of two colliding spherical nuclei can be represented as parametrized functions, e.g. in the Woods-Saxon (WS) potential form:

$$\begin{aligned} V^V(r) &= V_0^V f_{r_V,a_V}(r), \\ W^V(r) &= V_0^W f_{r_W,a_W}(r), \\ f_{r_0,a_0}(r) &= \frac{1}{1 + \exp\left(\frac{r-r_0}{a_0}\right)}, \end{aligned} \tag{7}$$

where V_0 is the depth of the potential, r_0 is the average distance, and a_0 is the diffusion parameter.

The Coulomb term has been taken as the interaction of a point-charge with a uniformly charged sphere

$$V^C(r) = \begin{cases} \frac{Z_1 Z_2 e^2}{2r_C}\left(3 - \frac{r^2}{r_C^2}\right), & \text{for } r \le r_C, \\ \frac{Z_1 Z_2 e^2}{r}, & \text{for } r > r_C. \end{cases}$$

The volume term of the OP can also be obtained by means of the DF model. Using the density distribution function of the nuclear matter of ^{6}Li (1), the double folding potential can take the following form:

$$V^V(r) = N_{r,i} V^{DF}(r)$$

$$V^{DF}(\mathbf{r}) = \int \int d\mathbf{r}_\alpha d\mathbf{r}_{Li} \, \rho_\alpha(\mathbf{r}_\alpha) \, V_{nn}(r_{\alpha Li}) \, \rho_{Li}(\mathbf{r}_{Li}). \tag{8}$$

where $r_{\alpha Li} = |\mathbf{r} + \mathbf{r}_\alpha - \mathbf{R}|$, the density distribution function of the α-projectile ρ_α can have the same shape as in Eq. (4). The $N_{r,i}$ normalization parameters are usually fitted to elastic scattering data in accordance with the dynamics of nuclear reaction. The V_{nn} effective nucleon-nucleon interactions are the sum of three Yukawa potentials, i.e. M3Y-potentials. The M3Y-potentials usually have the form:

$$V_{nn}(r) = \sum_{i=1}^{3} N_i \frac{\exp(-\mu_i r)}{\mu_i r}. \tag{9}$$

The parameters N_i, μ_i of the NN-potential can be taken in the M3Y-Paris parametrization, which are in Ref. [18].

Results and discussions

The density distribution function

A distinctive feature of the obtained results is the extended tail of the density function for the ^{6}Li nucleus in Figure 1. This is caused by the properties of valence nucleons in the three-body system. In particular, the density function of the core ρ_α tends to zero rapidly as the radius r increases in comparison with the nucleon density function ρ^N.

The main contribution to the density functions beginning from $r \simeq 3.0 \; fm$ is due to two valence nucleons. Another point in the behaviour of the density function ρ_N is the maximum at $r \simeq 1.8 \; fm$. In particular, the bump of ^{6}Li is sufficiently remarkable. This feature of the function explains that valence nucleons move away from the center of mass.

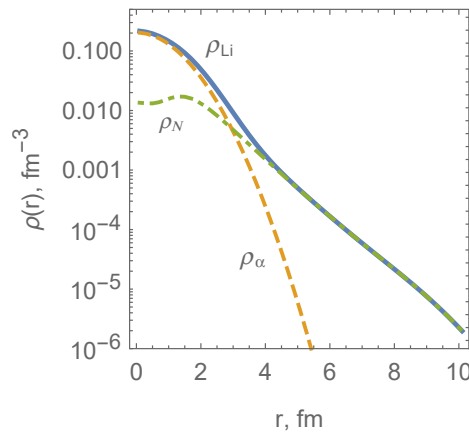Figure 1. The components of the density distribution function of the nuclear matter of ^{6}Li calculated within the three body model. The solid, dashed, and dot-dashed curves correspond to the total (ρ_{Li}), α-cluster (ρ_α), and np-cluster (ρ_N) density functions, respectively.
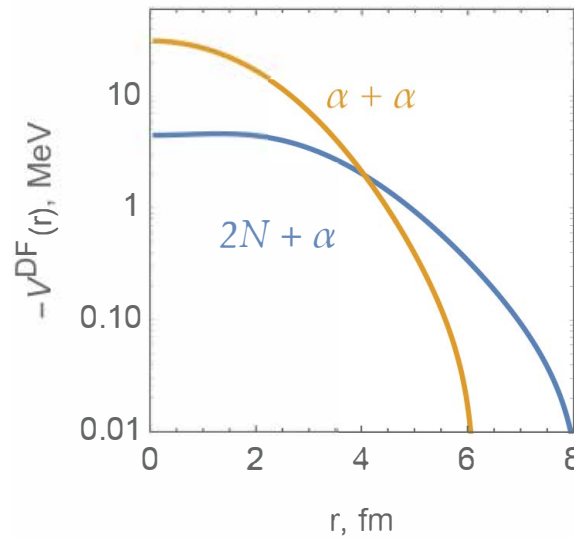
Figure 2. The folding potential $V^{DF}(r)$ calculated with the density functions of the nuclear matter of ^{6}Li. The $\alpha + \alpha$ designation is for the $V^{DF}_{\alpha+\alpha}$ potential, while $2N + \alpha$ is for the $V^{DF}_{2N+\alpha}$ potential.

Elastic scattering

To calculate the elastic scattering cross section, we used the DF potential with the density depended DDM3Y-Paris effective NN-potential [18]. The three body density functions of nuclear matter were used to calculate the potential. Due to the additive feature of the density function, it is possible to look into the interaction of the α-projectile with the clusters inside the nucleus ^{6}Li:

$$V^{DF}(r) = V^{DF}_{\alpha+\alpha}(r) + V^{DF}_{2N+\alpha}(r) \tag{10}$$

In Figure 2, the function of the interaction potential $V^{DF}_{\alpha+\alpha}(r)$ of the α-projectile with the α-cluster rapidly tends to zero, while the function of the interaction potential of the α-projectile with the np-cluster slowly decreases. It should also be noted that starting from the distance $r \simeq 4.0$ the main contribution is due to the interaction of the projectile with the np-cluster.

The folding potential was chosen to be the real part of the optical potential with the N_r fitting parameter. As regards the imaginary part, the same shape of the real part was used but with the parameters N_i. The Woods-Saxon potential with six parametrizations was taken from [11] for comparison with the DF potential. The theoretical curves based on the DF and WS potentials show good agreement with experimental data. It should be noted that the DF potential for the elastic scattering $\alpha + {}^6$Li reaction depends only on two parameters in contrast to the WS potential which depends on six parameters.

The calculated differential cross section performed in the OM framework describes well the experimental data except the backward scattering angles. The potential parameters used in the OM calculations are listed in Table 1.
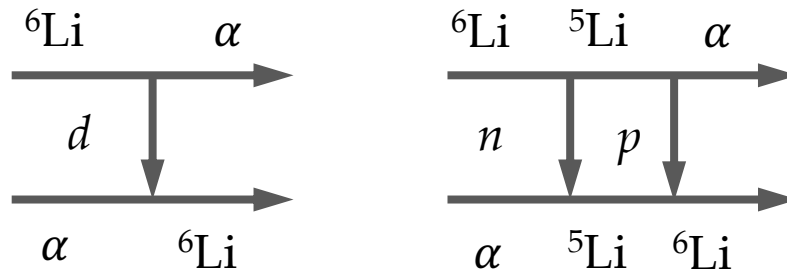
Figure 3. Schematic representation of the elastic transfer nuclear reaction, on the left - one-step, on the right - two-step transfer mechanisms.

Elastic transfer

The rising of the elastic scattering cross section starting from $90°$ suggests the existence of additional reaction mechanisms. In this case, in order to register the same particle as the elastically scattered projectile, the np-cluster must be transferred to the target at the backward angles. The transfer mechanisms of the nuclear reaction $\alpha + {}^6Li \rightarrow {}^6Li + \alpha$ are shown schematically in Figure 3.

The differential cross section of the transfer reactions is calculated within the CRC method by means of the *FRESCO* code [19]. For the nuclear reaction $\alpha + {}^6Li \rightarrow {}^6Li + \alpha$ the differential cross section can be written as follows

$$\frac{d\sigma}{d\Omega}(\theta) = |f(\theta)_{OM} + f_{one-step}(\pi - \theta) + f_{two-step}(\pi - \theta)|^2, \qquad (11)$$

where the amplitude $f_{one-step}$ is the amplitude of the finite-range transfer, and $f_{two-step}$ is the amplitude of the two-step transfer mechanism (see, e.g. [17, 19]).

The input and output channel potentials were taken as a double folding potential, and the optical potential with global optical parametrizations was chosen for α particles in the intermediate channel [20]. The calculations have shown that the cross sections depend insignificantly on the selected potential for the intermediate channel. The wave functions of the bound states were chosen by fitting the potential depth to the binding energies of the composite systems.

The results of calculating the differential cross section of the elastic collision of the $\alpha + {}^6Li$ system and the results of calculations for the elastic transfer are shown in Figures 4 and 5. The mechanism of elastic collision in the nuclear reaction prevails over other mechanisms at the forward scattering angles. However, starting from $90°$ it can be seen that the main contribution to the cross section is caused by the one-step transfer of np-cluster of ${}^6Li$.

In Figure 5, the one-step transfer dominates over the two-step transfer mechanism by one order of magnitude at the backward scattering angles. That makes

Table 1.
The parameters of the potentials used in OM calculations for thr $\alpha + {}^6Li$ nuclear reaction. For more details, see the text.

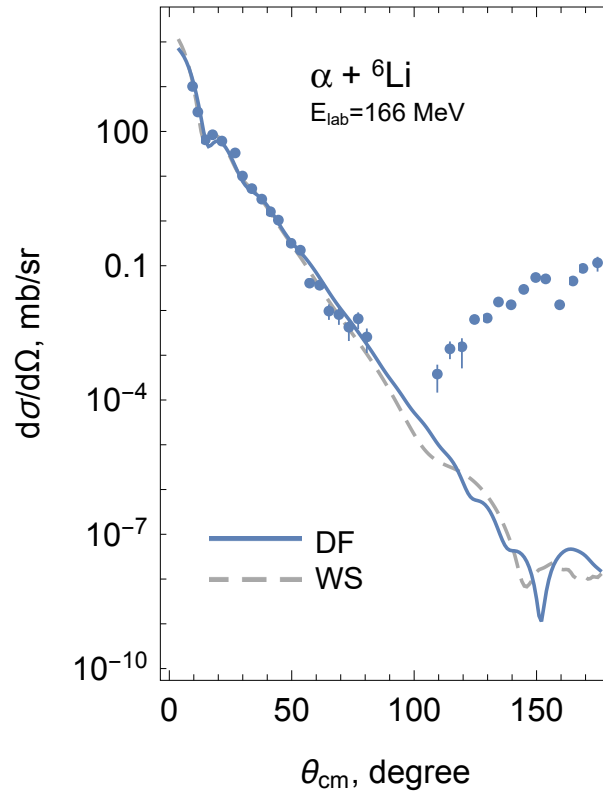|	$-V_0$, MeV	R_v, fm	a_v, fm	$-W_0$, MeV	R_w, fm	a_w, fm	χ^2/N
DF		N_r=2.0			N_i=1.8		11.61
WS	102.5	1.78	0.820	11.8	4.11	0.950	15.43

Figure 4. The differential cross section of the elastic scattering of ^{6}Li by α-particles at $E_{lab} = 166$ MeV with the different potentials: the double folding potential DF (blue solid), the WS (gray dashed) [11]. Experimanetal data are taken from [11].
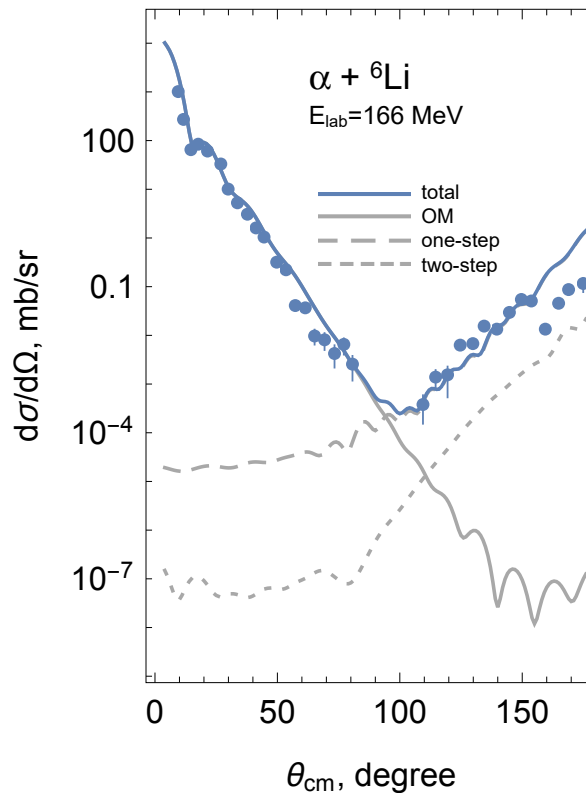

Figure 5. The cross sections of the elastic transfer reaction are represented in terms of the transfer mechanisms: elastic scattering (solid gray), one-step transfer (gray dashed), two-step transfer of np-cluster (dotted) and their coherent sum (solid blue). Experimental data are from Ref. [11].

total sense since the np-cluster is less bound than n: $E_{BE}(d) = 1.5$ MeV and $E_{BE}(n) = 5.7$ MeV. The best agreement with the experimental data is obtained if one uses the spectroscopic amplitudes for the configuration $2S_1 \simeq 0.7$, and for the configuration $2D_1 \simeq 0.5$. The obtained results based on the CRC calculations are in good agreement with the experimental data.

Conclusions

The nucleus ^{6}Li was theoretically investigated in terms of the cluster structure on the example of the α particle elastic scattering at 166 MeV. The nucleus under study is suggested to be the three body system $\alpha + p + n$. This conception is fixed by applying the three body wave function based on the Gaussian functions. The three body wave function was used in order to obtain the density distribution function of the nuclear matter of ^{6}Li. The density distribution function was implemented in the Double-folding model calculations. The DF potential made it possible to look into the interaction of the α-projectile withe clusters of ^{6}Li.

The obtained DF potential can describe the elastic scattering data with two parameters. Taking into account the proposed mechanisms of the np-cluster, it was possible to get good agreement of the calculated differential cross section with the available data in the full range of scattering angles.

References

[1] V.I. Kukulin et al., Nucl. Phys. A **453** (1987) 365-388. [*CrossRef*]
[2] K. Varga, Y. Suzuki, Phys. Rev. C **52** (1995) 2885-2905. [*CrossRef*]
[3] M. Zhukov et al., Phys. Rep. **231** (1993) 151-199. [*CrossRef*]
[4] A. Gnech et al., Phys. Rev. C **102** (2020) 014001. [*CrossRef*]
[5] B.R. Barrett, et el., Prog. Part. Nucl. Phys. **69** (2013) 131-181. [*CrossRef*]
[6] A. Shirokov et al., Phys. Lett. B **644** (2007) 33-37. [*CrossRef*]
[7] A. Kasparov et al., Bull. Russ. Acad. Sci.: Phys. **85** (2021) 534-537. [*CrossRef*]
[8] A. Amar, A.A. Ibraheem, Int. Jour. Mod. Phys. E **30** (2021) 2150090. [*CrossRef*]
[9] N. Burtebayev, et al., Phys. At. Nucl. **73** (2010) 746-756. [*CrossRef*]
[10] S. Sakuta et al., Phys. At. Nucl. **72** (2009) 1982. [*CrossRef*]
[11] Y.T. Oganessian et al., Phys. Rev. C **60** (1999) 044605. [*CrossRef*]
[12] B.A. Urazbekov et al., Bull. Russ. Acad. Sci.: Phys. **81** (2017) 690-694. [*CrossRef*]
[13] B.A. Urazbekov et al., Eur. Jour. Phys. Funct. Mat. **2** (2018) 17-22. [*CrossRef*]
[14] B.A. Urazbekov et al., Phys. At. Nucl. **84** (2021) 250-255. [*CrossRef*]
[15] B.A. Urazbekov et al., Act. Phys. Pol. B Proc. Suppl. **14** (2021) 799-809. [*CrossRef*]
[16] G.R. Satchler, W. G. Love, Phys. Rep. **55** (1979) 183-254. [*CrossRef*]
[17] G.R. Satchler, Direct nuclear reactions (Oxford, Clarendon Press, 1983) 854 p.
[18] N. Anantaraman et al., Nucl. Phys. A **398** (1983) 269-278. [*CrossRef*]
[19] I.J. Thompson, Comp. Phys. Rep. **7** (1988) 167-212. [*CrossRef*]
[20] V. Avrigeanu et al., Phys. Rev. C **49** (1994) 2136-2141. [*CrossRef*]